Author/s:
Zhou, W;Menkhorst, E;Dimitriadis, E

Title:
Jagged1 regulates endometrial receptivity in both humans and mice

Date:
2021-08-01

Citation:
Zhou, W., Menkhorst, E. & Dimitriadis, E. (2021). Jagged1 regulates endometrial receptivity in both humans and mice. FASEB Journal, 35 (8), https://doi.org/10.1096/fj.202100590R.

Persistent Link:
https://hdl.handle.net/11343/278740

Article type : Research Article

Title: Jagged1 regulates endometrial receptivity in both humans and mice

Authors: Wei Zhou[1,2], Ellen Menkhorst [1,2], Evdokia Dimitriadis [1,2]*

Affiliations: [1]Department of Obstetrics and Gynaecology, University of Melbourne, Parkville, Victoria, 3010 Australia.

[2]Gynaecology Research Centre, Royal Women's Hospital, Parkville, Victoria, 3052 Australia.

***Corresponding author:** Evdokia Dimitriadis, Level 7, The Royal Women's Hospital, 20 Flemington Road, Parkville, Victoria, 3052 Australia. Ph: + 61 3 9594 4392; Email: eva.dimitriadis@unimelb.edu.au.

Running title: Jagged1 regulates endometrial receptivity

Nonstandard abbreviations:

Bmp2: Bone morphogenetic protein 2
Cldn: Claudin
Cox2: Cyclooxygenase-2
DLL: Delta like
DMEM: Dulbecco's modified eagle medium
DPP4: Dipeptidyl peptidase 4
Erbb3: Erb-B2 receptor tyrosine kinase 3
ESR1: Estrogen receptor alpha
F11r: F11 receptor
FBS: Fetal bovine serum
Foxo1: Forkhead box protein O1

Gadd45a:	Growth arrest and DNA damage-inducible protein GADD45 alpha
Gdf15:	Growth/differentiation factor 15
GPX3:	Glutathione peroxidase 3
HEECs:	Primary human endometrial epithelial cells
HES1:	Hairy and enhancer of split homolog 1
HEY1:	Hairy/enhancer-of-split related with YRPW motif protein 1
IGFBP1:	Insulin-like growth factor-binding protein 1
ITGB3:	Integrin beta 3
JAG:	Jagged
Lamc2:	Laminin subunit gamma 2
LIFR:	Leukemia inhibitory factor receptor
MAOA:	Monoamine oxidase A
MAML:	Mastermind-like protein
Ncam1:	Neural cell adhesion molecule 1
NICD:	Notch intracellular domain
NOTCH:	Neurogenic locus notch homolog protein
Ocln:	Occludin
PBS:	Phosphate-buffered saline
PGR:	Progesterone receptor
P-STAT3:	Phosphorylated signal transducer and activator of transcription 3
RBPJ:	Recombination signal binding protein for immunoglobulin kappa J region
SPP1:	Secreted phosphoprotein 1
TBS:	Tris-buffered saline
Tgfb2:	Transforming growth factor beta 2

Abstract

The human endometrium undergoes cycle dependent changes and is only receptive to an implanting blastocyst within a narrow window of 2-4 days in the mid-secretory phase. Such functional changes require delicate interplay between a diversity of factors including cytokines and signaling pathways. The Notch signaling pathway members are expressed in human endometrium. We have previously demonstrated that Notch ligand Jagged1 (JAG1) localizes in the endometrial luminal epithelium (LE) and is abnormally reduced in infertile women during receptivity. However, the functional consequences of reduced JAG1 production on endometrial receptivity to implantation of the blastocyst are unknown. This study aimed to determine the role of JAG1 in regulating endometrial receptivity in humans and mice. Knockdown of *JAG1* in both primary human endometrial epithelial cells and Ishikawa cells significantly reduced their adhesive capacity to HTR8/SVneo (trophoblast cell-line) spheroids. We confirmed that in human endometrial epithelial cells, JAG1 interacted with Notch Receptor 3 (NOTCH3) and knockdown of *JAG1* significantly reduced the expression of Notch signaling downstream target *HEY1* and classical receptivity markers. Knockdown of *Jag1* in mouse LE significantly impaired blastocyst implantation. We identified ten genes (related to tight junction, infertility and cell adhesion) that were differentially expressed by *Jag1* knockdown in LE in mice. Further analysis of the tight junction family members in both species revealed that JAG1 altered the expression of tight junction components only in mice. Together, our data demonstrated that JAG1 altered endometrial epithelial cell adhesive capacity and regulated endometrial receptivity in both humans and mice likely via different mechanisms.

Keywords: endometrial receptivity, blastocyst implantation, JAG1, Notch pathway, endometrial epithelial cell

Introduction

Dysregulated or disrupted endometrial receptivity is one of the leading causes for implantation failure and a significant bottleneck for IVF treatment (1, 2). It is well established that during most stages of the menstrual cycle, the human endometrium is at a state of low receptivity and only receptive to an implanting blastocyst within a narrow window of 2-4 days in the mid-secretory phase (3). It is during this time period blastocysts can adhere to the luminal epithelium of the endometrium initiating implantation (4). Recent single cell sequencing on human endometrium across the menstrual cycle has identified an abrupt and discontinuous transcriptomic activation in the epithelia in the mid-secretory phase (5). Such transcriptomic and accordingly functional changes in the mid-secretory phase require a delicate interplay between a diversity of factors including hormones, cytokines and signaling pathways.

Adding to this complexity is that blastocyst implantation is a dynamic process. As an initial step of implantation, the blastocyst first adheres to the surface luminal epithelium. This is quickly followed by a firm attachment by increasing the interactions between luminal epithelium and the trophectoderm cells of the blastocyst. Once firmly attached, the blastocyst breaches the luminal epithelial cells and invades into the stomal layer of the endometrium (4). In response to this process, the endometrial luminal epithelium accordingly undergoes morphological and molecular changes. Notable examples include tight junctions which increase in depth and tightness at the lateral surface of luminal epithelial cells to maintain an epithelial structure and control signaling transduction between cells for the preparation of blastocyst attachment (6-8). However, downregulation of tight junction proteins is observed at the implantation site in mice likely to facilitate the invasion of the blastocyst (7).

The Notch signaling pathway has been involved in the regulation of cell proliferation, adhesion, invasion, and apoptosis via cell-cell interactions (9). Canonical Notch signaling is activated when a Notch ligand on an adjacent cell membrane binds with a receptor on the target cell, resulting in the release of the intracellular domain of the Notch receptor (NICD). Bioactive NICD translocates to the nucleus where it activates the transcription of Notch target genes via interactions with other Notch coactivators (Mastermind-like protein [MAML] and immunoglobulin kappa J region [RBPJ]) (9, 10). Mammalian Notch signaling has four receptors (NOTCH1-4) and five ligands (Delta-like [DLL]1, 3, 4 and Jagged [JAG]1, 2) which generally co-exist in cells with well-controlled coordination (9). Although ligand binding generally leads to the cleavage of Notch receptor and subsequent release of NICD, different ligand and receptor interactions often elicit diverse downstream functional outputs (11). This is confirmed via a binding site profile comparison between NOTCH1 and NOTCH2 in the same pancreatic cancer cells using chromatin immunoprecipitation sequencing (12). Less than 10% of the binding sites are common between NOTCH1 and NOTCH2 (12).

Notch receptors and ligands are expressed in the human endometrium (10, 13-15). Single cell sequencing analyses of human endometrium across the menstrual cycle have revealed an increased expression of NOTCH3 in the epithelial cells specifically in the receptive window (5), suggesting that Notch signaling may play essential roles in regulating endometrial receptivity. Functional studies in mice have discovered that abnormal Notch signaling leads to multiple uterine defects including impaired decidualization, absence of uterine glands and inhibition of progesterone signaling (16, 17). Our previous study has identified that JAG1 expression is significantly increased in the luminal epithelium in the mid-secretory phase, compared to proliferative phase of fertile endometrium (18). A comparison of JAG1 expression in the luminal epithelium between endometrium collected from fertile and infertile women revealed a significant decrease in the infertile group (18).

To the best of our knowledge, however, the functional consequences of lower expression of JAG1 on endometrial receptivity and blastocyst implantation are not addressed. *Jag1* null mice are embryonic lethal and die at Embryonic day (E)11.5, therefore their fertility is unknown (19). Conditional knockout of JAG1 in mouse endothelial cells blocks endothelial-to-mesenchymal transition (20) which is a similar process to plasma membrane transformation (6) which occurs in the endometrial luminal epithelium during the receptive phase to facilitate blastocyst implantation. The aim of this study was to investigate whether dysregulation of JAG1 affects endometrial receptivity. We explored whether knockdown of *JAG1* affects the adhesive capacity of human endometrial epithelial cells *in vitro*. We utilized a mouse model to determine the overall effects of *Jag1* knockdown in the uterine luminal epithelial cells on blastocyst implantation *in vivo*. Moreover, changes of key molecular targets in response to *JAG1* knockdown between humans and mice were compared.

Materials and Methods

Ethics

Human endometrial tissue: Written informed consent was obtained from each patient and the study was approved by the Human Research Ethics Committee at Monash Health (ID: #03066B) and the Royal Women's Hospital (SSA1813). Mouse experiment: All experimental procedures involving animals were conducted with the approval of the Animal Ethics Committee at the University of Melbourne (project ID: 1814657).

Reagents and cell line

Unless otherwise stated, chemicals were purchased from Sigma-Aldrich (St. Louis, MO, USA) and were of molecular biology or research grade. Details of the primary and secondary antibodies used throughout this study are summarized in Supplemental Table 1. Rabbit IgG isotype control (#X0903) was from DAKO (Glostrup, MUN, Denmark). Collagenase was purchased from Worthington (CLS-3, Lakewood, NJ, USA). *In vitro* transfection reagents (*JAG1* siRNA mimic, scrambled control, Lipofectamine RNAiMAX, Opti-MEM Reduced serum medium) were supplied by Thermo (Waltham, MA, USA). Cell culture reagents (Dulbecco's Modified Eagle Medium [DMEM]: Nutrient Mixture F-12, Roswell Park Memorial Institute 1640 Medium, L-glutamine, penicillin/streptomycin, Fetal Bovine Serum [FBS]) were from Thermo. 2'OMe modified and cholesterol conjugated *Jag1* siRNA (5' GAAGGAACAACCUGUAAUA dTdT 3', 3' dTdT CUUCCUUGUUGGACAUUAU 5') and scrambled control were obtained from RiboBio (Guangzhou, China). SuperScript™ III First-Strand Synthesis System (18080-051) and SYBR Green Master Mix (4367659) were from Thermo. 4–15% precast polyacrylamide gel was purchased from BIO-RAD (Hercules, CA, USA). RIPA protein lysis buffer was from Thermo (89900) and protease inhibitor cocktail Set III was purchased from Merck Millipore (#539134, Darmstadt, Germany). xCELLigence assay was conducted using the RTCA DP xCELLigence instrument (Noble Park, VIC, Australia). The Ishikawa cell line was provided by Dr M. Nishida (Tsukuba University, Tochigi, Japan). HTR8/SVneo trophoblast cell line (CRL-3271) was purchased from the ATCC and cultured as in the manufacturer's instruction.

Endometrial tissue collection and primary endometrial epithelial cells isolation

All women (26-42 years of age) that consented had regular menstrual cycles (28–32 day cycles), were not using intrauterine contraceptives and had not used hormones for at least 3 months before surgery. The endometrial tissue samples were collected by curettage and were from the functionalis layer. The collected endometrium were examined by experienced gynecological pathologists to confirm the cycle stage and absence of endometrial dysfunction. Primary human endometrial epithelial cells (HEECs) were isolated from normal human endometrium, as we previously published (21). Briefly, endometrial tissue was finely chopped and digested at 37 °C for 40 min with collagenase (727 μg/mL, 262 units) and Dnase I (25 μg/mL) diluted in Phosphate-buffered saline (PBS) containing 0.36 mM calcium chloride. Suspension was then filtered through 43 μm nylon mesh to remove stromal cell contamination and remaining cells and epithelial fragments were collected, resuspended and plated appropriately into a 96 well plate. As stromal cells attached quicker than epithelial fragments, cells and epithelial fragments were cultured for 30 min (twice) to remove any stromal cell contamination. Unattached epithelial fragments were collected and cultured to harvest HEECs.

In vivo mouse experiments

Adult female mice (C57BL6/J, 8-16 weeks old) were mated to male mice (8-52 weeks old). The morning of plug detection was defined as E0. 10 µg (20 µL) Ago*Jag1* siRNA or scrambled control were delivered into the uterine horn via intrauterine injection at E3. Ago*Jag1* siRNA (2’OMe modified and cholesterol conjugated) was delivered in saline as recommended by the manufacturer. To confirm the successful delivery, mouse uteri were collected at E4 (prior to implantation) and the luminal epithelium was separated from the uteri via Dispase (0.5% in Hank's Balanced Salt Solution) digestion for 2 h at room temperature (22). The purity of luminal epithelium isolated using enzyme digestion has been confirmed by previous studies in which the histological appearance of the isolated luminal epithelium and contamination for stromal cells were examined (23, 24). The isolated luminal epithelium was used for qPCR and immunoblotting to determine JAG1 expression. Implantation sites were recorded and collected at E4.5, the time of implantation (via tail vein injection of 100 µL 1% Chicago blue dye) (25). Uteri were also collected on E4 and E4.5 for other downstream analysis.

In vitro siRNA transfection

Ishikawa cells or HEECs at 70-80% confluency were transfected with Lipofectamine RNAiMAX and Opti-MEM medium containing 20 nM *JAG1* siRNA, *MAML1* siRNA or scrambled control according to the manufacturer's instructions. After 24 h, transfection medium was replaced with fresh culture medium (antibiotic-free) and cells were cultured for 48 h before being subjected to spheroid adhesion assay or other downstream analysis.

Spheroid adhesion assay

Spheroids were generated using HTR8/SVneo trophoblast cells to mimic blastocyst attachment, as we previously published (26-28). Briefly, 2000 HTR8/SVneo cells/well were plated into wells of a U-shaped, ultra-low attachment 96 well plate. Cells were then cultured for 48 h to form spheroids before spheroids were collected and transferred to transfected HEEC or Ishikawa cell monolayer (20 spheroids/well of 96 well plate) to initiate spheroid adhesion assay. After a 2 h (HEECs) or 4 h (Ishikawa cells) incubation at 37°C, culture medium was removed and non-adherent spheroids removed by a gentle wash with 150 µL PBS/well. The remaining attached spheroids were counted, and the adhesive capacity of each well expressed as a percentage of the original spheroid number.

xCELLigence assay

xCELLigence assay was conducted to examine the real-time adhesive capacity of *JAG1* knockdown compared to scrambled control Ishikawa cells, as we previously described (29). This assay works by measuring the electrical flow transmission between gold microelectrodes embedded on each well of 96-well plate. Adhering cells disrupt the electrical transmission between electrodes and the impedance in flow is expressed as cell index and is positively correlated with cell adhesive capacity. Briefly, Ishikawa cells, transfected with 20 nM *JAG1* siRNA or a scrambled control were seeded in the xCELLigence 96 well E-plate at 10,000 cells per well in fresh culture medium supplemented with 5% FBS (30). The cell index was recorded every 15 min for 8 h, as a representation of adhesion and every 1 h following this for 72 h, as a representation of proliferation. Data were calculated using RTCA software 1.2, supplied with the instrument and exported for statistical analysis.

Immunohistochemistry and immunocytochemistry

Mouse uteri were fixed in 10% formalin, embedded in paraffin and sectioned at 4 µm thickness. Sections were then dewaxed, rehydrated, and subjected to antigen retrieval under optimized conditions: microwaving in 10 mM sodium citrate for 5 min (Phosphorylated signal transducer and activator of transcription 3 [P-STAT3] and cleaved-Caspase 3) (31) or 50 mM Tris (pH 10.5) for 10 min (NOTCH1 and NOTCH2). No antigen retrieval was required for JAG1 and DESMIN (32). Following antigen retrieval, endogenous peroxidase activity was blocked with 3% hydrogen peroxide diluted in methanol for 15 min at room temperature. Sections were then washed with Tris-buffered saline (TBS) and incubated in a non-immune blocking buffer (10% goat serum and 2% mouse serum in TBS) for 30 min at room temperature. Primary antibodies were diluted as instructed in Supplemental Table 1 and sections were incubated overnight at 4 °C. An isotype control was included with every tissue stained in which the non-immune antibody of the same IgG isotype was substituted for each primary antibody at the same concertation. These slides were then washed with TBS-Tween 0.6% (v/v) and positive signaling was revealed via the avidin-biotin-diaminobenzidine system. Sections were counterstained with hematoxylin to indicate cell nuclei. Slides were then mounted with DPX and imaged using an Olympus light microscope. For immunocytochemistry staining of Ishikawa cell cultures, transfected cells were fixed in 4% paraformaldehyde for 15 min and permeabilized by incubation in 0.1% Triton X-100 for 10 min. After PBS wash, cells were treated with 3% hydrogen peroxide and immunolabeled as described for uterine sections.

RNA isolation and RT-qPCR

For Ishikawa cells and HEECs, cells were lysed with TRI Reagent and RNA was isolated according to the manufacturer's protocol and treated with TURBO DNAfree Kit to remove genomic DNA contamination. Mouse uterine luminal epithelial RNA was isolated using Qiagen RNeasy Mini Kit and genomic DNA contamination was removed using Qiagen RNase-free DNase set. After isolation, 300 ng total RNA was converted to cDNA using Thermo SuperScript™ III First-Strand Synthesis System. qPCR was performed on the Applied Biosystems ViiA7 system as follows: 95 °C for 10 min and 40 cycles of 95 °C for 15 s followed by 60 °C for 1 min. Gene expression was normalized to *18S*. Relative expression levels were calculated using the comparative cycle threshold method (ΔΔCt). Primer sequences used in this study are provided in Supplemental Table 2.

Customized RT^2 Profiler PCR array

We selected 83 genes from predesigned arrays available from QIAGEN, including those for female fertility (PAMM-164Z), extracellular matrix and adhesion molecules (PAMM-013Z) and epithelial to mesenchymal transition (PAMM-090Z). PCR array was conducted on the Applied Biosystems ViiA7 system, according to the manufacturer's instructions. *18s* was used for gene expression normalization. Combating batch effect (ComBat) was used to remove the batch effect among different array plates before statistical analysis.

Protein extraction and Immunoblotting

Mouse uterine luminal epithelium, transfected Ishikawa cells and HEECs were lysed in RIPA buffer for protein extraction. Insoluble material was pelleted by centrifugation (17,000 × g, 15 min, 4°C) and the soluble proteins were quantified using a bicinchoninic acid protein assay kit. For immunoblotting, equal amounts of protein were loaded on 4–15% precast polyacrylamide gel and then transferred to polyvinylidene difluoride membranes (pre-soaked with methanol). Membranes were blocked with 5% skim milk in TBS for 1 h and incubated with primary antibody prepared in 5% skim milk. After washing three times with TBS-Tween 0.1% (v/v), membranes were incubated with appropriate horse radish peroxidase (HRP)-conjugated secondary antibodies. After additional washes in TBS-Tween 0.1% (v/v), labeled proteins were detected using a chemiluminescence kit. For quantification, appropriate bands were assessed by densitometry, normalized against a loading control GAPDH, as previously described (33).

Statistics

All experiments were replicated a minimum of 3 times with replicate numbers indicated in figure legends. Statistical analyses were performed using PRISM 8.0 and paired student's t-test or repeated measures ANOVA was used for statistical analysis with a significance threshold of $P < 0.05$. Data were presented as the mean ± SEM.

Results

Knockdown of *JAG1* reduces the adhesive capacity of human endometrial epithelial cells *in vitro*.

As JAG1 strongly localizes to the endometrial luminal epithelium during the mid-secretory phase of the menstrual cycle (18) (Supplemental Figure 1), we investigated whether JAG1 regulated the cell adhesive capacity of human endometrial epithelial cells. Primary human endometrial epithelial cells (HEECs) and Ishikawa cells were used to assess the functional consequences of *JAG1* knockdown on epithelial cell adhesion. qPCR analysis first confirmed the successful knockdown of *JAG1,* with *JAG1* mRNA expression showed a significant decrease ($P < 0.05$) in *JAG1* siRNA treated group compared to control, in both HEECs and Ishikawa cells (Figure 1A). The localization of JAG1 in Ishikawa cells was also examined as it has not been determined before. A conserved membrane and cytoplasm staining was recorded as was seen in human endometrial tissue (Figure 1B and Supplemental Figure 1). In addition, the *JAG1* siRNA treated group had much lower staining intensity, compared to control, confirming the knockdown of JAG1 protein. Functional analysis via spheroid adhesion assays in both *in vitro* models identified that *JAG1* knockdown in epithelial cells significantly impaired ($P < 0.05$) their adhesiveness to HTR8/SVneo spheroids (Figure 1C). Transfected Ishikawa cells were also subjected to xCELLigence to examine adhesive capacity of Ishikawa cells in real-time after *JAG1* siRNA transfection. As shown in Figure 1D, Ishikawa cells treated with *JAG1* siRNA experienced a significant reduction ($P < 0.05$) of cell adhesion within 3 h after seeding and up to 8 h of culture. Ishikawa cell proliferation was significantly reduced by *JAG1* knockdown after 80 h of culture compared to control ($P < 0.0001$, Supplemental Figure 2).

Knockdown of *JAG1* in human endometrial epithelial cells affects the expression of receptivity markers via Notch dependent and independent pathways

We further investigated the potential mechanisms by which JAG1 regulates endometrial epithelial cell adhesive capacity. As a ligand of the Notch pathway, we confirmed that *JAG1* knockdown significantly reduced the expression of classical Notch target gene Hairy/enhancer-of-split related with YRPW motif protein 1 (*HEY1*) ($P < 0.01$), however Hairy and enhancer of split homolog 1 (*HES1*) was not affected (Figure 2A). Seven endometrial receptivity markers were also selected for analysis. As shown in Figure 2B, the expression of five genes including Leukemia inhibitory factor receptor (*LIFR*), Secreted phosphoprotein 1 (*SPP1*), Integrin beta 3 (*ITGB3*), Monoamine oxidase A (*MAOA*) and Insulin-like growth factor-binding protein 1 (*IGFBP1*) were significantly reduced after *JAG1* knockdown, compared to control while the expression of Glutathione peroxidase 3 (*GPX3*) and Dipeptidyl peptidase 4 (*DPP4*) was not altered (Figure 2C). Progesterone receptor (PGR) and Estrogen receptor alpha (ESR1) are important regulators of endometrial receptivity and blastocyst implantation (34). We confirmed that the reduced expression of receptivity markers listed above was likely not via *PGR* and *ESR1* as *JAG1* knockdown did not significantly change the expression of these two hormone receptors compared to control (Figure 2D). To determine if the regulation of these markers was via Notch dependent or independent pathways, we conducted siRNA transfection to knockdown the expression of a Notch pathway coactivator, *MAML1* in Ishikawa cells. qPCR confirmed the knockdown of *MAML1* ($P < 0.001$; Figure 2E). Among the five receptivity markers that were regulated by JAG1, only *SPP1* mRNA expression levels were significantly reduced by *MAML1* knockdown compared to control ($P < 0.05$; Figure 2F) (28).

JAG1 interacts with NOTCH3 in human endometrial epithelial cells.

Notch signaling is achieved via Notch ligand binding to Notch cell surface receptors and intracellular release of the Notch intracellular domain (NICD) (9). To determine which receptor(s) may interact with JAG1 to initiate Notch signaling, we used antibodies that can recognize the NICD of each Notch receptor and applied immunoblotting and densitometry analysis to quantify the changes in NICD production between *JAG1* siRNA treated and control groups. We confirmed knockdown of JAG1 protein after JAG1 siRNA transfection compared to control ($P < 0.05$, Figure 3A). Densitometry analysis of each Notch NICD identified that NOTCH3 NICD was significantly decreased ($P < 0.05$) in response to *JAG1* knockdown (Figure 3A). Unexpectedly, NOTCH1 and NOTCH2 NICD were significantly increased in response to *JAG1* knockdown (Figure 3A). We further confirmed that in HEECs, the expression of NOTCH3 NICD was decreased after *JAG1* knockdown (Figure 3B), compared to control.

JAG1 regulates uterine receptivity and blastocyst implantation *in vivo* in mice.

Having secured evidence that knockdown of *JAG1* compromised endometrial epithelial cell adhesion, we used mice as an *in vivo* model to investigate the consequences of *Jag1* knockdown on endometrial receptivity and implantation. We first revealed that prior to implantation, JAG1 localized on the apical membrane and extended into the apicolateral cell border in the uterine luminal epithelium (Figure 4A). To explore whether *Jag1* knockdown compromised blastocyst implantation *in vivo*, Ago*Jag1* or control siRNA was injected into each side of the mouse uterine horn at E3 so that each mouse had a treatment and control uterine horn (Figure 4B). qPCR analysis on E4 uterine luminal epithelium (early in the morning, prior to implantation) confirmed that intrauterine injection of Ago*Jag1* siRNA significantly decreased *Jag1* mRNA expression, compared to control ($P < 0.01$, Figure 4C). The successful knockdown of JAG1 was further confirmed at the protein level via immunoblotting ($P < 0.01$, Figure 4D). Treated mice uteri were also collected at E4.5 and the number of implantation sites was visualized via Chicago blue dye injection and recorded. There was a significant reduction ($P < 0.05$) in the number of implantation sites in the uterine horns that were transfected with Ago*Jag1* siRNA compared to control (Figure 4E).

To assess the effect of *Jag1* knockdown on receptivity markers, E4 uterine luminal epithelium from both Ago*Jag1* siRNA and control treated groups were subjected to qPCR (35-38). Prior to assessment, the expression of classical Notch target genes (*Hey1* and *Hes1*) and Notch receptors and ligands were determined using E4 luminal epithelium treated with either Ago*Jag1* siRNA or control. We confirmed that *Jag1* knockdown affected Notch signaling by demonstrating a significant reduction of the expression of *Hes1* ($P < 0.05$), but not *Hey1* (Figure 5A), which was opposite to our observations in the human model (Figure 2A). qPCR analysis also identified that knockdown of *Jag1* significantly reduced the expression of receptivity markers Forkhead box protein O1 (*Foxo1*), *Lifr* and *Stat3*, compared to control (Figure 5B). The expression of *Pgr* and *Esr1* was also determined by qPCR. No significant difference was found for *Pgr* expression after Ago*Jag1* siRNA treatment, compared to control which is similar to the human models. However, *Esr1* expression was significantly decreased after Ago*Jag1* siRNA treatment (Figure 5C). To further determine the effects on implantation, Chicago blue dye was used to identify implantation sites at E4.5. For Ago*Jag1* siRNA treated E4.5 uteri, we randomly selected areas with no signs of implantation and investigated implantation and decidualization markers by immunohistochemistry. In areas positive for

Chicago blue dye, a local post-implantation decidual response was evident by DESMIN staining and Phosphorylated STAT3 (P-STAT3) staining was observed surrounding the blastocyst implantation site in the control (Figure 5D). *Jag1* knockdown significantly reduced the expression of decidualization genes Bone morphogenetic protein 2 (*Bmp2*) and Cyclooxygenase-2 (*Cox2*) ($P < 0.05$, Figure 5E) in the uteri compared to control confirming that the blastocyst failed to firmly attach to initiate implantation and the decidualization response. As implantation sites were found in uteri of two mice treated with Ago*Jag1* siRNA (n=1 implantation site/uterus) (Figure 4E), we determined if there were any defects in the decidualization response in the implantation sites. DESMIN and P-STAT3 was recorded in the implantation sites and there was no apparent difference in the extent of staining compared to control (Figure 5D). In addition, Ago*Jag1* siRNA treatment did not lead to apoptosis in the attached blastocyst or luminal epithelium as no positive staining of cleaved-Caspase 3 was revealed in either of the treatment groups. Mouse spleen served as a positive control for cleaved-Caspase 3 expression and showed positive staining (Figure 5F). However, the implantation chamber did not appear to form properly in implantation sites found in uteri treated with Ago*Jag1* siRNA (n=2, Figure 5F), with the implantation chamber in Ago*Jag1* siRNA treated uteri showing impaired closure compared to implantation sites from the same mice in the control uterine horn (n=2, Figure 5F).

JAG1 regulates the expression of tight junction components in mice

We next performed a customized RT^2 Profiler PCR array to identify *Jag1* gene targets in mouse uterine luminal epithelium at E4. This array selected 83 genes from predesigned arrays related to female fertility, extracellular matrix and adhesion molecules and epithelial to mesenchymal transition (Supplemental Dataset). Among the 83 gene targets, Ago*Jag1* siRNA treatment significantly decreased the expression of seven genes; Claudin 4 (*Cldn4*), Growth arrest and DNA damage-inducible protein GADD45 alpha (*Gadd45a*), *Esr1*, Erb-B2 Receptor Tyrosine Kinase 3 (*Erbb3*), F11 receptor (*F11r*), Neural cell adhesion molecule 1 (*Ncam1*) and Laminin subunit gamma 2 (*Lamc2*) while the expression of three genes namely *Gpx3*, Transforming growth factor beta 2 (*Tgfb2*) and Growth/differentiation factor 15 (*Gdf15*) was increased significantly compared to that for the control uterine horn (Table 1). CLDN4 is a component of lateral tight junctions that are upregulated in the luminal epithelium during the receptive phase in both humans and mice (6). We confirmed the reduction in *Cldn4* following *Jag1* knockdown in the mouse uterine luminal epithelium ($P < 0.05$) (Figure 6A). However, production of *CLDN4* was not regulated by *JAG1* knockdown in HEECs and Ishikawa cells (Supplemental Figure 3), suggesting *Cldn4* is a unique target of JAG1 in mice. We further examined the expression of other tight junction components after *JAG1* knockdown in both humans and mice. qPCR revealed that *Cldn1* and *Ocln* were significantly downregulated after *Jag1* siRNA treatment only in the mouse uterine luminal epithelium (Figure 6A, Supplemental Figure 3), but there was no effect in human cells.

The expression of JAG1 in the mouse uterine luminal epithelium was compared before and after implantation by immunohistochemistry. JAG1 was expressed evenly in the luminal epithelium before implantation at E4 and this expression was reduced specifically in the luminal epithelium in contact with the attached blastocyst in the implantation chamber at E4.5 (Figure 6B) where tight junctions are no longer required in order to facilitate blastocyst invasion. Among four Notch receptors, NOTCH3 and NOTCH4 deficient female mice are fertile (39, 40) as such they are not essential for blastocyst implantation in mice. We examined NOTCH1 and NOTCH2 via immunohistochemistry. A similar staining pattern was recorded for NOTCH1 but not NOTCH2, with the level specifically reduced in the luminal epithelium surrounding the implantation chamber at E4.5 compared to other regions of the luminal epithelium (Figure 6B, Supplemental Figure 4).

Discussion

In this study, we identify that JAG1 regulates endometrial adhesive capacity and receptivity in both humans and mice. For human models, we applied both HEECs and Ishikawa cells. *JAG1* knockdown in both cells significantly impaired their adhesive capacity to trophoblast cell formed spheroids *in vitro*. *JAG1* knockdown reduced Notch signaling via NOTCH3 and dysregulated a number of receptivity markers in human endometrial epithelial cells. The functional consequences of *JAG1* knockdown on blastocyst implantation are verified in mice. Here we confirm that *JAG1* knockdown in mice impaired uterine receptivity and blastocyst implantation. Using a target screen array, we identified a number of receptivity markers affected by *JAG1* knockdown. Surprisingly, tight junction genes were regulated by *Jag1* only in mice.

JAG1 belongs to the Notch signaling pathway which is involved in the regulation of a wide range of cellular processes including cell adhesion, invasion and differentiation (41). As a Notch ligand, JAG1 signals to recipient cells expressing Notch receptors. JAG1 can signal to equivalent or different cell types suggesting that the Notch signaling pathway in the uterine luminal epithelial cells can be activated via ligand binding from adjacent luminal epithelial cells and also from trophectoderm cells at the time of blastocyst attachment. The former is likely the case in the mouse uterus as *Jag1* knockout embryos die at E11.5 but show apparent normal implantation (19). In support in humans, our xCELLigence data using endometrial epithelial cells alone demonstrates that JAG1 regulates their adhesive capacity. This is supported by our previous study in which we identified all four Notch receptors in human endometrial epithelial cells indicating that they may act via Notch receptors in adjacent endometrial epithelial cells (13).

A recent single cell sequencing study on human endometrium has determined a gene expression profile that can define the window of implantation. Entrance into the window of implantation is featured with an abrupt and discontinuous transcriptomic activation in the unciliated epithelial cells (5). Notably, NOTCH3 is the only Notch receptor that identified with an increased expression when reaching the implantation window (5). *JAG1* knockdown led to decreased expression of NOTCH3 NICD in our study suggesting that compared to other Notch ligands and receptors, JAG1-NOTCH3 may play a dominant role in regulating endometrial receptivity in humans. Increased expression of NOTCH1 and NOTCH2 NICD after *JAG1* knockdown was not able to compensate for the loss of NOTCH3 NICD. In contrast, NOTCH3 may not be involved in regulating endometrial receptivity in mice as NOTCH3 deficient female mice are fertile (39). Rather, NOTCH1 has been revealed with important roles in regulating female fertility in mice. NOTCH1 deficient embryos die between E10 and 12 (42). Loss/gain of function studies reveal that the deletion of *Notch1* in mice impairs decidualization and leads to implantation failure (17, 43). By contrast, overexpression of Notch1 NICD via *Pgr*-Cre in mouse uterus impairs uterine development and fertility (16). Our investigation of NOTCH1 expression in the uterine luminal epithelium has identified an even distribution before implantation and a reduction specifically in the implantation chamber right after implantation suggesting NOTCH1 may be required in the mouse uterus to ensure normal uterine function and fertility. One recent study offers important mechanistic insights into NOTCH1 regulating uterine functions. It demonstrates that NOTCH1 knockout specifically in the mouse uterus via *Pgr*-Cre generally affects genes enriched for cell-cell and cell-matrix interaction, cell adhesion and plasma membrane function (44). This is consistent with some of our findings where we noted gene expression levels in these pathways were significantly changed after *Jag1* knockdown in the mouse uterine luminal epithelium.

It is likely that Notch receptors define the Notch pathway downstream targets in the signaling receiving cells. Our data revealed that JAG1 interacted with different Notch receptors between human and mouse models. In the mouse uterus, NOTCH1 NICD rather than NOTCH3 NICD expression was decreased in the luminal epithelium in contact with the implanting blastocyst, where JAG1 expression was decreased. A previous study has compared the binding site profiles between NOTCH1 and NOTCH2 in human pancreatic cancer cells. A total of 598 binding sites are identified for NOTCH1 and 745 for NOTCH2 with only 49 of them being common targets between these two Notch receptors (12). It is likely that tight junction components are regulated via JAG1-NOTCH1 pathway in the mouse uterine epithelial cells. Consistent with this idea, it has been shown that in human intestinal epithelial cells, knockdown of *NOTCH1* similarly impairs the formation of tight junctions via the downregulation of Claudin 5 and Occludin (45). Immunohistochemical staining of human endometrial tissue reveals that tight junction proteins are expressed in endometrial epithelial cells and some components such as CLDN1 and CLDN4 show an increased expression in the secretory phase compared to proliferative phase suggesting an involvement in receptivity (46). The decreased expression of NOTCH3 NICD caused by *JAG1* knockdown in human endometrial epithelial cells did not affect the expression of the tight junction components investigated. We remain uncertain if stromal cells contribute to the regulation of tight junctions via JAG1 as our *in vitro* human models use endometrial epithelial monolayer. Endometrial epithelial – stromal cell interactions are known to be important in receptivity as stromal cells express a high level of PGR in the mid-secretory phase (47) and tight junctions are regulated by progesterone (46). To the best of our knowledge, however, there is presently no evidence linking stromal cells to a role in regulating tight junctions in the luminal epithelium. Although tight junction components were not regulated by JAG1 in our human models, it is likely that molecules related to cell adhesion are affected as xCELLigence revealed a change in cell adhesion while up to 60 h, cell proliferation was not impaired by *JAG1* knockdown.

In mice, once the implantation chamber is formed, the attached blastocyst and surrounding epithelial layer increase in length to create gaps in the epithelium to facilitate invasion (48, 49). The formation of the implantation chamber is triggered by the decidual swellings (50) and certainly requires the morphogenetic adjustment of the luminal epithelium surrounding the attached blastocyst. Our study has revealed two replicates of mice that went on to develop a single implantation site at E4.5. However, the implantation chamber was not formed properly, compared to control treated groups from the same mice. Immunohistochemistry staining of decidualization marker DESMIN did not appear to show any abnormalities in these implantation sites. Similar defects in uterine luminal closure have also been identified in uterine *RBPJ* knockout mice (51). In this model, deletion of *Rbpj* enhances the estrogen response and impairs the on-time uterine luminal closure by increasing epithelial cell proliferation (51). Further analysis reveals that the regulation is via Notch-independent mechanisms as co-transfection of a dominant-negative form of the other Notch coactivator, MAML1 does not reduce the estrogen response to RBPJ (51). It is likely that the mechanisms leading to impaired luminal closure are different in our study as *Jag1* knockdown in the uterine luminal epithelium significantly reduced the expression of *Esr1* which was not seen in the previous study (51).

Our recent study has revealed that knockdown of *MAML1* in Ishikawa cells impairs their adhesive capacity (28). This alteration in adhesion likely does not occur via alterations in the levels of the steroid hormone receptors PGR and ESR1 which is consistent with our observations in *JAG1* siRNA treated Ishikawa cells. Both *JAG1* and *MAML1* siRNA treatments only reduced the expression of *HEY1*, but not *HES1* (28), indicating similar downstream effects of the Notch dependent pathway. To investigate whether the regulation of receptivity markers by JAG1 was via Notch dependent or independent pathways, *MAML1* siRNA was transfected into Ishikawa cells to determine the effects on the expression of genes associated with receptivity. Among five receptivity markers that were significantly altered by *JAG1* knockdown, only *SPP1* was altered by *MAML1* and *JAG1* knockdown (28), suggesting the effects of the other four receptivity genes were not via Notch dependent pathway as knockdown of the Notch dependent pathway coactivator *MAML1* did not impact the expression of those genes. The regulation of *SPP1* by the Notch dependent pathway has been confirmed by other studies (52, 53) and *SPP1* contains an RBPJ binding site 723-734 base pair relative to its transcription start site suggesting the capability of direct interaction with Notch coactivator complex in the promoter region to initiate transcription.

In our functional models, *JAG1* siRNA treatment did not completely block human spheroid attachment or mouse blastocyst implantation. This is in accordance with the partial knockdown of *JAG1* mRNA in human endometrial epithelial cells and mouse uterine luminal epithelium. Although immunoblotting showed a further decrease of JAG1 at the protein level compared to the mRNA expression levels, there was no complete knockout of *JAG1*. We remain uncertain if knockout of *JAG1* would completely block spheroid adhesion / blastocyst implantation. From clinical samples examined however, we observe very low levels of JAG1 in the infertile endometrial luminal epithelium (immunostaining intensity value of ~0.2), compared to fertile endometrium (staining intensity value of ~2.6) during receptivity, although immunostaining does not measure the concentration of proteins so we cannot be certain of the concentration of JAG1 in endometrium of women with infertility (18).

Altogether, our study has provided evidence that JAG1 is essential to maintain endometrial epithelial cell adhesive capacity and knockdown of *JAG1* affects endometrial receptivity and blastocyst implantation in mice. Such functional roles are in accordance with the observation that JAG1 production is abnormally reduced in the infertile human endometrium during receptivity. JAG1 may interact with different Notch receptors and function via different mechanisms between humans and mice to regulate endometrial receptivity. This study stimulates further investigation into the potential of using JAG1 as a novel molecular target to assist with the diagnosis of endometrial receptivity.

Acknowledgments

The authors are grateful to Sr. Emily-Jane Bromley for orchestrating the tissue collection and the women who donated the endometrial tissue used in this study. This work was supported by a project grant and a senior research fellowship from the National Health and Medical Research Council (NHMRC) of Australia to ED. WZ was supported by an Early Career Researcher Grant (University of Melbourne). EM was supported by a NHMRC project grant and a Department of Obstetrics and Gynaecology Mid-Career Researcher Fellowship (University of Melbourne).

Conflict of Interest

The authors report no conflict of interest.

Author Contributions

W. Zhou conducted the experiments and drafted the manuscript. E. Menkhorst assisted with the xCELLigence assay and data analysis and contributed to manuscript editing. E. Dimitriadis conceived and designed the study, contributed to data interpretation and analysis, and manuscript preparation and review.

References

1. Fatemi, H., and Popovic-Todorovic, B. (2013) Implantation in assisted reproduction: a look at endometrial receptivity.

Reprod Biomed Online **27**, 530-538

2. Craciunas, L., Gallos, I., Chu, J., Bourne, T., Quenby, S., Brosens, J. J., and Coomarasamy, A. (2019) Conventional and modern markers of endometrial receptivity: a systematic review and meta-analysis. *Hum Reprod Update* **25**, 202-223
3. Evans, J., Salamonsen, L. A., Winship, A., Menkhorst, E., Nie, G., Gargett, C. E., and Dimitriadis, E. (2016) Fertile ground: human endometrial programming and lessons in health and disease. *Nat Rev Endocrinol* **12**, 654-667
4. Norwitz, E. R., Schust, D. J., and Fisher, S. J. (2001) Implantation and the survival of early pregnancy. *N Engl J Med* **345**, 1400-1408
5. Wang, W., Vilella, F., Alama, P., Moreno, I., Mignardi, M., Isakova, A., Pan, W., Simon, C., and Quake, S. R. (2020) Single-cell transcriptomic atlas of the human endometrium during the menstrual cycle. *Nat Med* **26**, 1644-1653
6. Whitby, S., Zhou, W., and Dimitriadis, E. (2020) Alterations in Epithelial Cell Polarity During Endometrial Receptivity: A Systematic Review. *Front Endocrinol* **11**, 596324
7. Wang, X., Matsumoto, H., Zhao, X., Das, S. K., and Paria, B. C. (2004) Embryonic signals direct the formation of tight junctional permeability barrier in the decidualizing stroma during embryo implantation. *J Cell Sci* **117**, 53-62
8. Satterfield, M. C., Dunlap, K. A., Hayashi, K., Burghardt, R. C., Spencer, T. E., and Bazer, F. W. (2007) Tight and adherens junctions in the ovine uterus: differential regulation by pregnancy and progesterone. *Endocrinology* **148**, 3922-3931
9. Bray, S. J. (2016) Notch signalling in context. *Nat Rev Mol Cell Biol* **17**, 722-735
10. Cuman, C., Menkhorst, E., Winship, A., Van Sinderen, M., Osianlis, T., Rombauts, L. J., and Dimitriadis, E. (2014) Fetal–maternal communication: the role of Notch signalling in embryo implantation. *Reproduction* **147**, 75-86
11. Kopan, R., Chen, S., and Liu, Z. (2014) Alagille, Notch, and robustness: why duplicating systems does not ensure redundancy. *Pediatr Nephrol* **29**, 651-657
12. Liu, H., Zhou, P., Lan, H., Chen, J., and Zhang, Y.-x. (2017) Comparative analysis of Notch1 and Notch2 binding sites in the genome of BxPC3 pancreatic cancer cells. *J Cancer* **8**, 65-73
13. Van Sinderen, M., Cuman, C., Gamage, T., Rainczuk, K., Osianlis, T., Rombauts, L., and Dimitriadis, E. (2014) Localisation of the Notch family in the human endometrium of fertile and infertile women. *J Mol Histol* **45**, 697-706
14. Mazella, J., Liang, S., and Tseng, L. (2008) Expression of Delta-like protein 4 in the human endometrium. *Endocrinology* **149**, 15-19
15. Cobellis, L., Caprio, F., Trabucco, E., Mastrogiacomo, A., Coppola, G., Manente, L., Colacurci, N., De Falco, M., and De Luca, A. (2008) The pattern of expression of Notch protein members in normal and pathological endometrium. *J Anat* **213**, 464-472
16. Su, R.-W., Strug, M. R., Jeong, J.-W., Miele, L., and Fazleabas, A. T. (2016) Aberrant activation of canonical Notch1 signaling in the mouse uterus decreases progesterone receptor by hypermethylation and leads to infertility. *Proc Natl Acad Sci U S A* **113**, 2300-2305
17. Afshar, Y., Jeong, J.-W., Roqueiro, D., DeMayo, F., Lydon, J., Radtke, F., Radnor, R., Miele, L., and Fazleabas, A. (2012) Notch1 mediates uterine stromal differentiation and is critical for complete decidualization in the mouse. *FASEB J* **26**, 282-294
18. Cuman, C., Menkhorst, E., Rombauts, L., Holden, S., Webster, D., Bilandzic, M., Osianlis, T., and Dimitriadis, E. (2013) Preimplantation human blastocysts release factors that differentially alter human endometrial epithelial cell adhesion and gene expression relative to IVF success. *Hum Reprod* **28**, 1161-1171
19. Xue, Y., Gao, X., Lindsell, C. E., Norton, C. R., Chang, B., Hicks, C., Gendron-Maguire, M., Rand, E. B., Weinmaster, G., and Gridley, T. (1999) Embryonic lethality and vascular defects in mice lacking the Notch ligand Jagged1. *Hum Mol Genet* **8**,

723-730

20. Hofmann, J. J., Briot, A., Enciso, J., Zovein, A. C., Ren, S., Zhang, Z. W., Radtke, F., Simons, M., Wang, Y., and Iruela-Arispe, M. L. (2012) Endothelial deletion of murine Jag1 leads to valve calcification and congenital heart defects associated with Alagille syndrome. *Development* **139**, 4449-4460

21. Dimitriadis, E., Robb, L., and Salamonsen, L. (2002) Interleukin 11 advances progesterone-induced decidualization of human endometrial stromal cells. *Mol Hum Reprod* **8**, 636-643

22. Ye, X., Herr, D. R., Diao, H., Rivera, R., and Chun, J. (2011) Unique uterine localization and regulation may differentiate LPA3 from other lysophospholipid receptors for its role in embryo implantation. *Fertil Steril* **95**, 2107-2113

23. Bigsby, R., Cooke, P., and Cunha, G. (1986) A simple efficient method for separating murine uterine epithelial and mesenchymal cells. *Am J Physiol* **251**, E630-E636

24. Campbell, E., O'hara, L., Catalano, R., Sharkey, A., Freeman, T., and Johnson, M. H. (2006) Temporal expression profiling of the uterine luminal epithelium of the pseudo-pregnant mouse suggests receptivity to the fertilized egg is associated with complex transcriptional changes. *Hum Reprod* **21**, 2495-2513

25. Luu, K. C., Nie, G. Y., and Salamonsen, L. A. (2004) Endometrial calbindins are critical for embryo implantation: evidence from in vivo use of morpholino antisense oligonucleotides. *Proc Natl Acad Sci U S A* **101**, 8028-8033

26. Zhou, W., Santos, L., and Dimitriadis, E. (2020) Characterization of the role for cadherin 6 in the regulation of human endometrial receptivity. *Reprod Biol Endocrinol* **18**, 1-10

27. Takamura, M., Zhou, W., Rombauts, L., and Dimitriadis, E. (2019) The long noncoding RNA PTENP1 regulates human endometrial epithelial adhesive capacity in vitro: implications in infertility. *Biol Reprod* **102**, 53-62

28. Zafir, S., Zhou, W., Menkhorst, E., Santos, L., and Dimitriadis, E. (2021) MAML1: a coregulator that alters endometrial epithelial cell adhesive capacity. *Fertil Res Pract* **7**, 1-11

29. Menkhorst, E., Griffiths, M., Van Sinderen, M., Rainczuk, K., Niven, K., and Dimitriadis, E. (2018) Galectin-7 is elevated in endometrioid (type I) endometrial cancer and promotes cell migration. *Oncol Lett* **16**, 4721-4728

30. George, L., Winship, A., Sorby, K., Dimitriadis, E., and Menkhorst, E. (2020) Profilin-1 is dysregulated in endometroid (type I) endometrial cancer promoting cell proliferation and inhibiting pro-inflammatory cytokine production. *Biochem Biophys Res Commun* **531**, 459-464

31. Winship, A. L., Koga, K., Menkhorst, E., Van Sinderen, M., Rainczuk, K., Nagai, M., Cuman, C., Yap, J., Zhang, J.-G., and Simmons, D. (2015) Interleukin-11 alters placentation and causes preeclampsia features in mice. *Proc Natl Acad Sci U S A* **112**, 15928-15933

32. Shuya, L. L., Menkhorst, E. M., Yap, J., Li, P., Lane, N., and Dimitriadis, E. (2011) Leukemia inhibitory factor enhances endometrial stromal cell decidualization in humans and mice. *PLoS One* **6**, e25288

33. Zhou, W., Anderson, A. L., Turner, A. P., De Iuliis, G. N., McCluskey, A., McLaughlin, E. A., and Nixon, B. (2017) Characterization of a novel role for the dynamin mechanoenzymes in the regulation of human sperm acrosomal exocytosis. *Mol Hum Reprod* **23**, 657-673

34. Cha, J., Sun, X., and Dey, S. K. (2012) Mechanisms of implantation: strategies for successful pregnancy. *Nat Med* **18**, 1754-1767

35. Cheng, J.-G., Chen, J. R., Hernandez, L., Alvord, W. G., and Stewart, C. L. (2001) Dual control of LIF expression and LIF receptor function regulate Stat3 activation at the onset of uterine receptivity and embryo implantation. *Proc Natl Acad Sci U S A* **98**, 8680-8685

36. Glasser, S. R., Lampelo, S., Munir, M. I., and Julian, J. (1987) Expression of desmin, laminin and fibronectin during in situ

differentiation (decidualization) of rat uterine stromal cells. *Differentiation* **35**, 132-142

37. Lee, K. Y., Jeong, J.-W., Wang, J., Ma, L., Martin, J. F., Tsai, S. Y., Lydon, J. P., and DeMayo, F. (2007) Bmp2 is critical for the murine uterine decidual response. *Mol Cell Biol* **27**, 5468-5478

38. Vasquez, Y. M., Wang, X., Wetendorf, M., Franco, H. L., Mo, Q., Wang, T., Lanz, R. B., Young, S. L., Lessey, B. A., and Spencer, T. E. (2018) FOXO1 regulates uterine epithelial integrity and progesterone receptor expression critical for embryo implantation. *PLoS Genet* **14**, e1007787

39. Krebs, L. T., Xue, Y., Norton, C. R., Sundberg, J. P., Beatus, P., Lendahl, U., Joutel, A., and Gridley, T. (2003) Characterization of Notch3‐deficient mice: Normal embryonic development and absence of genetic interactions with a Notch1 mutation. *Genesis* **37**, 139-143

40. Krebs, L. T., Xue, Y., Norton, C. R., Shutter, J. R., Maguire, M., Sundberg, J. P., Gallahan, D., Closson, V., Kitajewski, J., and Callahan, R. (2000) Notch signaling is essential for vascular morphogenesis in mice. *Genes Dev* **14**, 1343-1352

41. Tsakonas, S. A., Rand, M. D., and Lake, R. J. (1999) Notch signaling: cell fate control and signal integration in development. *Science* **284**, 770-776

42. Huppert, S. S., Le, A., Schroeter, E. H., Mumm, J. S., Saxena, M. T., Milner, L. A., and Kopan, R. (2000) Embryonic lethality in mice homozygous for a processing-deficient allele of Notch1. *Nature* **405**, 966-970

43. Afshar, Y., Miele, L., and Fazleabas, A. T. (2012) Notch1 is regulated by chorionic gonadotropin and progesterone in endometrial stromal cells and modulates decidualization in primates. *Endocrinology* **153**, 2884-2896

44. Wu, Y., He, J.-P., Xie, J., Wang, K.-z., Kang, J.-W., Fazleabas, A. T., and Su, R.-W. (2021) Notch1 is crucial for decidualization and maintaining the first pregnancy in the mouse. *Biol Reprod* **104**, 539-547

45. Dahan, S., Rabinowitz, K. M., Martin, A. P., Berin, M. C., Unkeless, J. C., and Mayer, L. (2011) Notch-1 signaling regulates intestinal epithelial barrier function, through interaction with CD4+ T cells, in mice and humans. *Gastroenterology* **140**, 550-559

46. Someya, M., Kojima, T., Ogawa, M., Ninomiya, T., Nomura, K., Takasawa, A., Murata, M., Tanaka, S., Saito, T., and Sawada, N. (2013) Regulation of tight junctions by sex hormones in normal human endometrial epithelial cells and uterus cancer cell line Sawano. *Cell Tissue Res* **354**, 481-494

47. Mote, P., Balleine, R., McGowan, E., and Clarke, C. (1999) Colocalization of progesterone receptors A and B by dual immunofluorescent histochemistry in human endometrium during the menstrual cycle. *J Clin Endocrinol Metab* **84**, 2963-2971

48. Ashary, N., Tiwari, A., and Modi, D. (2018) Embryo implantation: war in times of love. *Endocrinology* **159**, 1188-1198

49. Matsuo, I., and Hiramatsu, R. (2017) Mechanical perspectives on the anterior-posterior axis polarization of mouse implanted embryos. *Mech Dev* **144**, 62-70

50. Finn, C., and Hinchliffe, J. (1965) Histological and histochemical analysis of the formation of implantation chambers in the mouse uterus. *Reproduction* **9**, 301-309

51. Zhang, S., Kong, S., Wang, B., Cheng, X., Chen, Y., Wu, W., Wang, Q., Shi, J., Zhang, Y., and Wang, S. (2014) Uterine Rbpj is required for embryonic-uterine orientation and decidual remodeling via Notch pathway-independent and-dependent mechanisms. *Cell Res* **24**, 925-942

52. Villanueva, A., Alsinet, C., Yanger, K., Hoshida, Y., Zong, Y., Toffanin, S., Rodriguez–Carunchio, L., Solé, M., Thung, S., and Stanger, B. Z. (2012) Notch signaling is activated in human hepatocellular carcinoma and induces tumor formation in mice. *Gastroenterology* **143**, 1660-1669. e1667

53. Shen, Q., and Christakos, S. (2005) The vitamin D receptor, Runx2, and the Notch signaling pathway cooperate in the

transcriptional regulation of osteopontin. *J Biol Chem* **280**, 40589-40598

Table 1. Identification of significantly changed genes after *Jag1* knockdown in mouse uterine luminal epithelium via customized PCR gene array. **P* < 0.05, ***P* < 0.01.

Gene	**Significance (decreased after *Jag1* knockdown)**
Cldn4	**
Gadd45a	*
Esr1	*
Erbb3	**
F11r	*
Ncam1	*
Lamc2	*
Gene	**Significance (increased after *Jag1* knockdown)**
Gpx3	**
Tgfb2	*
Gdf15	*

Figure legends

Figure 1. *JAG1* knockdown compromises HEEC and Ishikawa cell adhesive capacity. A) HEECs (n=5) and Ishikawa cells (n=4) were transfected with either *JAG1* siRNA or scrambled control before functional analysis. Knockdown of *JAG1* was confirmed via qPCR. Gene expression was normalized to *18S*. B) Immunocytochemistry staining confirmed the successful knockdown of JAG1 in Ishikawa cells at the protein level, compared to control. An isotype control was included in which the non-immune antibody of the same isotype was substituted for the JAG1 antibody at the same concertation. C) Spheroid adhesion assay revealed that knockdown of *JAG1* in HEECs and Ishikawa cells both significantly compromised cell adhesive capacity, compared to control (n=5). D) xCELLigence analysis was conducted to examine the real-time adhesive capacity of *JAG1* knockdown compared to scrambled control Ishikawa cells (up to 8 h). Cell index is a measure of cell attachment. All data were presented as mean ± SEM. **P* < 0.05, ***P* < 0.01, ****P* < 0.001, *****P* < 0.0001.

Figure 2. *JAG1* knockdown in Ishikawa cells reduces Notch signaling activation and affects the expression of endometrial receptivity markers. A) qPCR analysis of classical Notch target genes (*HEY1* and *HES1*) identified that knockdown of *JAG1* in Ishikawa cells significantly reduced the expression of *HEY1* (n=7). B-C) qPCR analysis of seven endometrial receptivity markers revealed that *JAG1* knockdown in Ishikawa cells significantly reduced the expression of *LIFR*, *SPP1*, *ITGB3*, *MAOA* and *IGFBP1*. No significant changes were recorded for *GPX3* and *DPP4*. D) qPCR analysis of *PGR* and *ESR1* expression identified no significant changes after *JAG1* knockdown. E-F) qPCR analysis revealed that knockdown of a

Notch pathway coactivator, *MAML1* in Ishikawa cells did not affect the expression of *LIFR*, *ITGB3*, *MAOA* and *IGFBP1*. Expression levels were normalized to *18S* (n=6-7). All data were presented as mean ± SEM. **P* < 0.05, ***P* < 0.01, ns: no significant difference.

Figure 3. JAG1 interacts with NOTCH3 to activate Notch signaling in human *in vitro* models. A) After *JAG1* siRNA treatment in Ishikawa cells, the expression of all Notch receptors (cleaved intracellular region) in addition to JAG1was determined by immunoblotting and quantified by densitometry, normalized against a loading control GAPDH (n=3-4). Full length (FL) and the cleaved intracellular region (NICD) of each NOTCH receptor were indicated with arrows. Knockdown of JAG1 significantly decreased the expression of NOTCH3 NICD. However, the expression of NOTCH1 NICD and NOTCH2 NICD were significantly increased. B) Reduced expression of NOTCH3 NICD after *JAG1* knockdown was also confirmed in HEECs with *P* = 0.073 (n=3). All data were presented as mean ± SEM. **P* < 0.05, ***P* < 0.01, ns: no significant difference.

Figure 4. Knockdown of *Jag1* in the mouse uterus compromises blastocyst implantation *in vivo*. A) The immunolocalization of JAG1 was examined in the mouse uterus at E4 (n=3). JAG1 was localized on the apical membrane (black arrow) and extended to the apicolateral border of the luminal epithelial cells (yellow arrow). For clarity, the structure of luminal epithelium was outlined. An isotype control was included in which the non-immune antibody of the same isotype was substituted for the JAG1 antibody at the same concertation. B) Schematic of the intrauterine injection. *Jag1* siRNA or scrambled control was injected into each uterine horn at E3, so that each mouse has a siRNA and control treatment group. O: Ovary, F: Fallopian tube, U: Uterus. C) After injection, luminal epithelium and remaining uteri were collected at E4 and JAG1 expression was quantified via C) qPCR after normalization to *18s* (n=5) and D) immunoblotting after normalization to GAPDH (luminal epithelium, n=5). E) After injection, implantation sites (indicated with arrow heads) were recorded at E4.5 (n=5) via Chicago blue dye. *Jag1* knockdown in the mouse uterine luminal epithelium significantly reduced the number of implantation sites, compared to control. All data were presented as mean ± SEM. **P* < 0.05, ***P* < 0.01, ns: no significant difference.

Figure 5. Detection of Notch targets, uterine receptivity, decidualization and apoptosis markers in the mouse uteri treated with *Jag1* siRNA. After intrauterine injection of *Jag1* siRNA or control, mouse uterine luminal epithelium were collected at E4 (prior to implantation) and subjected to qPCR analysis to determine the expression of (A) classical Notch target genes (*Hey1* and *Hes1*, n=4), uterine receptivity markers (n=4) and hormone receptors (n=5). D-F) E4.5 (right after implantation) implantation sites were also collected for immunohistochemistry (D, F, n=2 as only two implantation sites were recorded from five treated mice; n=3 mice had no implantation sites after *Jag1* knockdown) and qPCR (E, n=3) to assess the expression of receptivity, decidualization and apoptosis markers. For qPCR, only areas with failed implantation (n=3) after *Jag1* siRNA treatment were assessed as only 2 replicates were available and were used for immunohistochemistry. Mouse spleen was used as a positive control for cleaved-Caspase 3

staining. For immunohistochemistry, an isotype control was included in which the non-immune antibody of the same isotype was substituted for each primary antibody at the same concertation. L: Lumen, *: Blastocyst. For qPCR analysis, expression levels were normalized to *18s*. Data were presented as mean ± SEM. *$P < 0.05$, **$P < 0.01$, ns: no significant difference.

Figure 6. *Jag1* knockdown dysregulates the expression of epithelial tight junction genes in the mouse uterine luminal epithelium. A) The expression of tight junction genes was examined by qPCR in mouse E4 luminal epithelium (LE) (n=5) that treated with either *JAG1* siRNA or control. A significant downregulation of *Cldn4, Cldn11 and Ocln* was recorded in the mouse uterine luminal epithelium uterine luminal epithelium that treated with *Jag1* siRNA, compared to control. Expression levels of all genes were normalized to *18s*. All data were presented as mean ± SEM. *$P < 0.05$, **$P < 0.01$, ns: no significant difference. B) The spatial expression of JAG1 and NOTCH1 was examined before (E4) and after (E4.5) blastocyst implantation in scrambled control treated mouse uterus. JAG1 localization was detected around the apical luminal border before implantation and this expression was reduced specifically in the luminal epithelium in contact with the attached blastocyst in the implantation chamber (outlined with yellow dotted lines) before invasion. Similarly, the level of NOTCH1 was specifically reduced in the luminal epithelium surrounding the implantation chamber (n=3). For isotype control, a non-immune antibody of the same isotype was substituted for each primary antibody at the same concertation. L: Lumen, *: Blastocyst.

Fig. 1

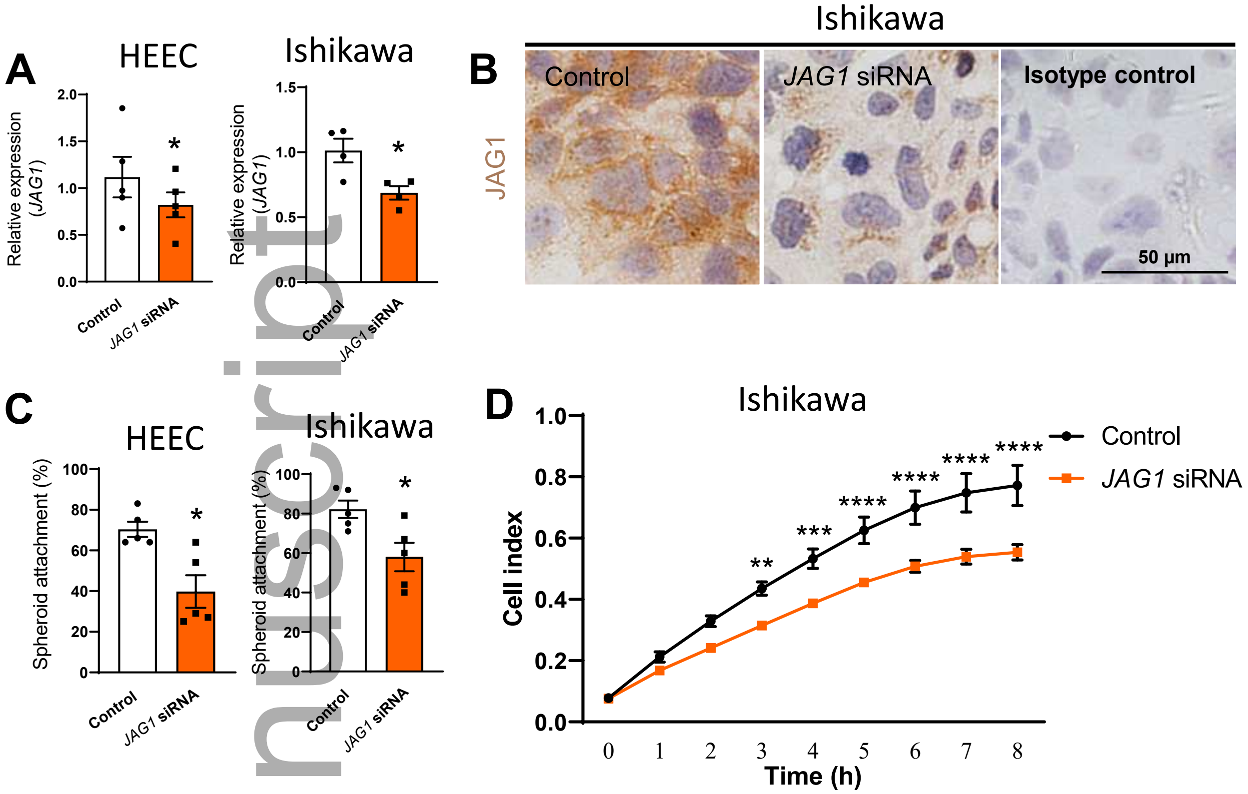
A
HEEC
Relative expression (JAG1)
2.0
1.5
1.0
0.5
0.0
*
Control
JAG1 siRNA
Ishikawa
Relative expression (JAG1)
1.5
1.0
0.5
0.0
*
Control
JAG1 siRNA
B
Ishikawa
JAG1
Control
JAG1 siRNA
Isotype control
50 µm
C
HEEC
Spheroid attachment (%)
100
80
60
40
20
0
*
Control
JAG1 siRNA
Ishikawa
Spheroid attachment (%)
100
80
60
40
20
0
*
Control
JAG1 siRNA
D
Ishikawa
Cell index
1.0
0.8
0.6
0.4
0.2
0.0
**
***
****
****
****
****
0
1
2
3
4
5
6
7
8
Time (h)
Control
JAG1 siRNA

Fig. 2

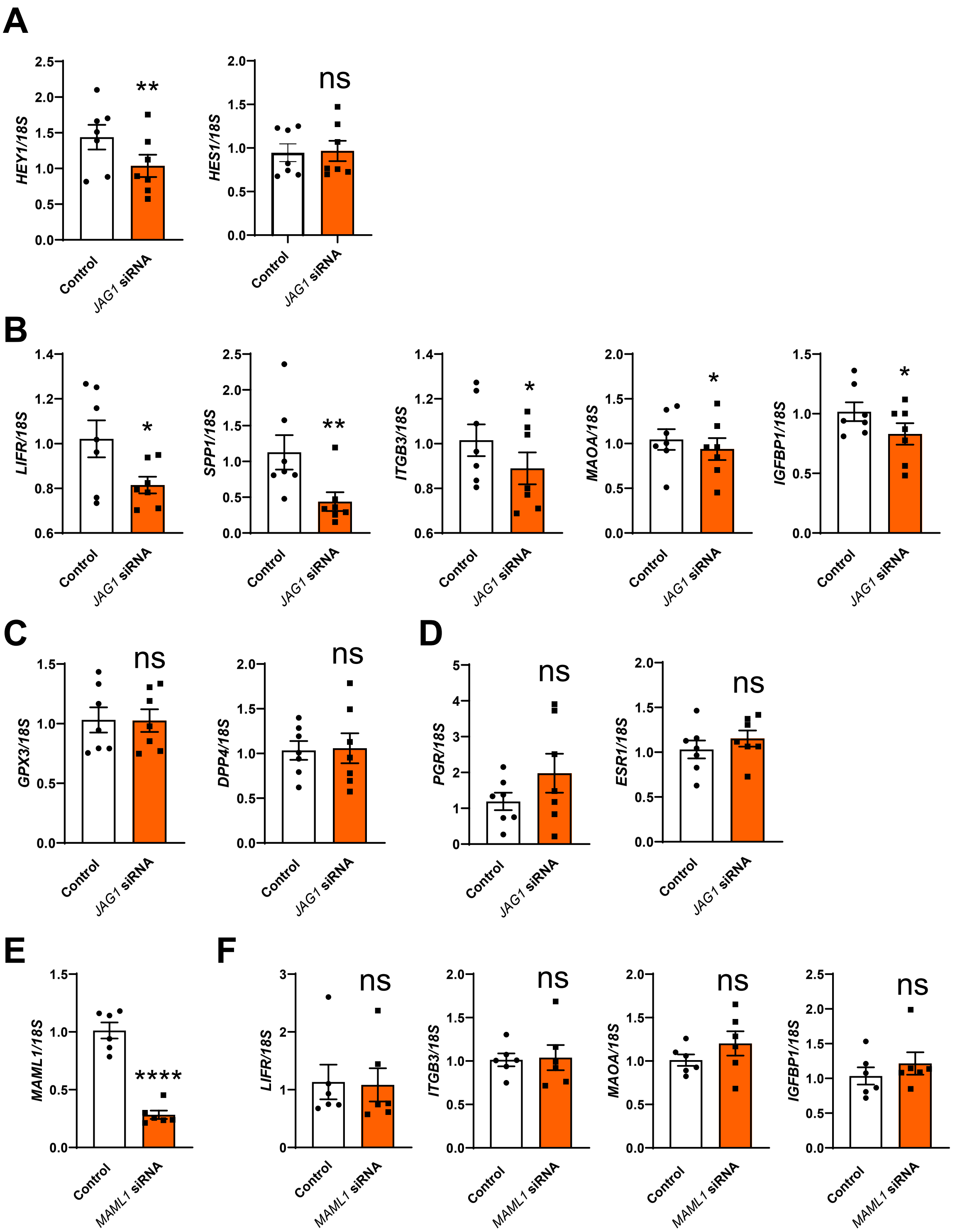
A
HEY1/18S
0.0
0.5
1.0
1.5
2.0
2.5
**
HES1/18S
0.0
0.5
1.0
1.5
2.0
ns
Control
JAG1 siRNA
B
LIFR/18S
0.6
0.8
1.0
1.2
1.4
*
SPP1/18S
0.0
0.5
1.0
1.5
2.0
2.5
**
ITGB3/18S
0.6
0.8
1.0
1.2
1.4
*
MAOA/18S
0.0
0.5
1.0
1.5
2.0
*
IGFBP1/18S
0.0
0.5
1.0
1.5
*
C
GPX3/18S
0.0
0.5
1.0
1.5
ns
DPP4/18S
0.0
0.5
1.0
1.5
2.0
ns
D
PGR/18S
0
1
2
3
4
5
ns
ESR1/18S
0.0
0.5
1.0
1.5
2.0
ns
E
MAML1/18S
0.0
0.5
1.0
1.5
****
Control
MAML1 siRNA
F
LIFR/18S
0
1
2
3
ns
ITGB3/18S
0.0
0.5
1.0
1.5
2.0
ns
MAOA/18S
0.0
0.5
1.0
1.5
2.0
ns
IGFBP1/18S
0.0
0.5
1.0
1.5
2.0
2.5
ns

Fig. 3

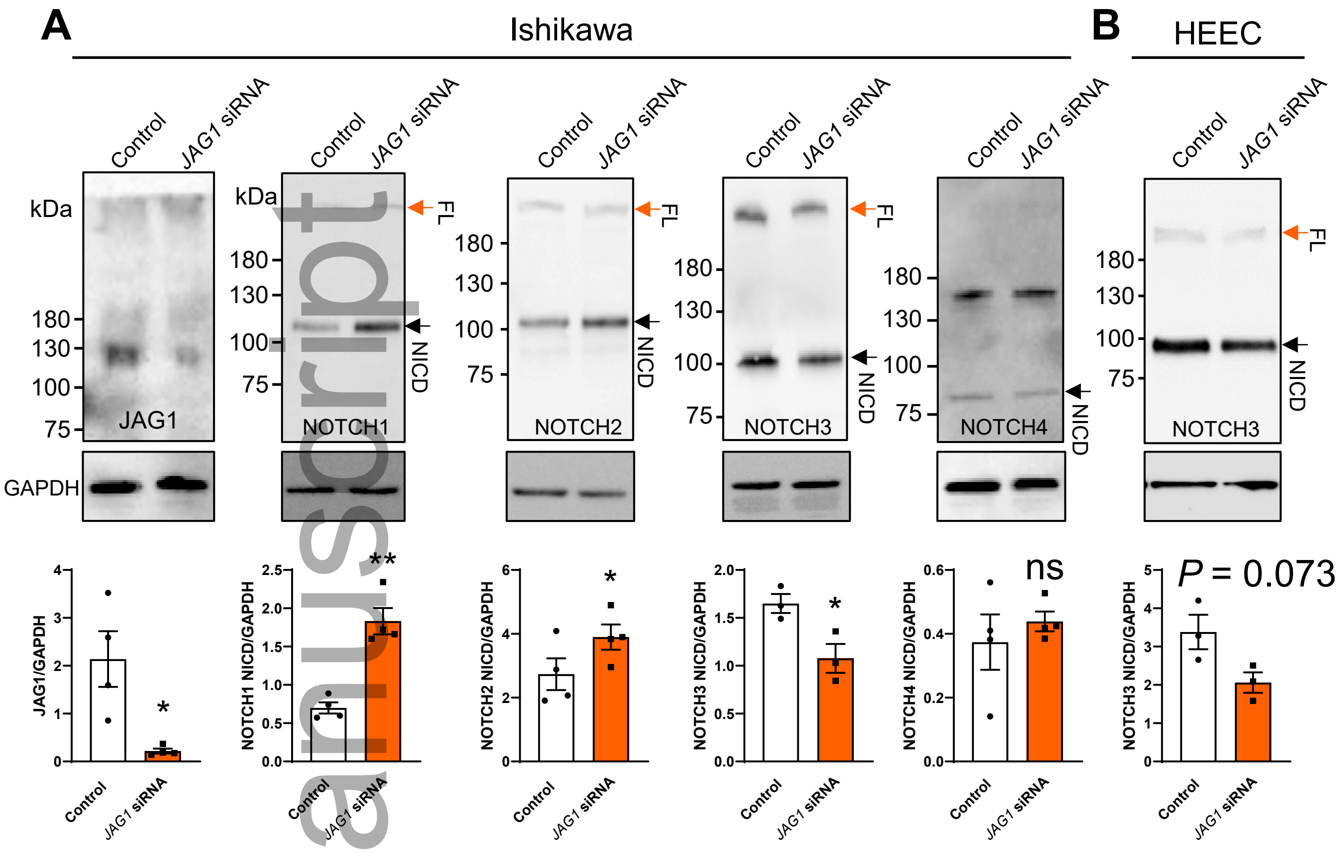
A
Ishikawa
B
HEEC
Control
JAG1 siRNA
kDa
180
130
100
75
JAG1
NOTCH1
NOTCH2
NOTCH3
NOTCH4
FL
NICD
GAPDH
JAG1/GAPDH
NOTCH1 NICD/GAPDH
NOTCH2 NICD/GAPDH
NOTCH3 NICD/GAPDH
NOTCH4 NICD/GAPDH
*
**
*
*
ns
P = 0.073

Fig. 4

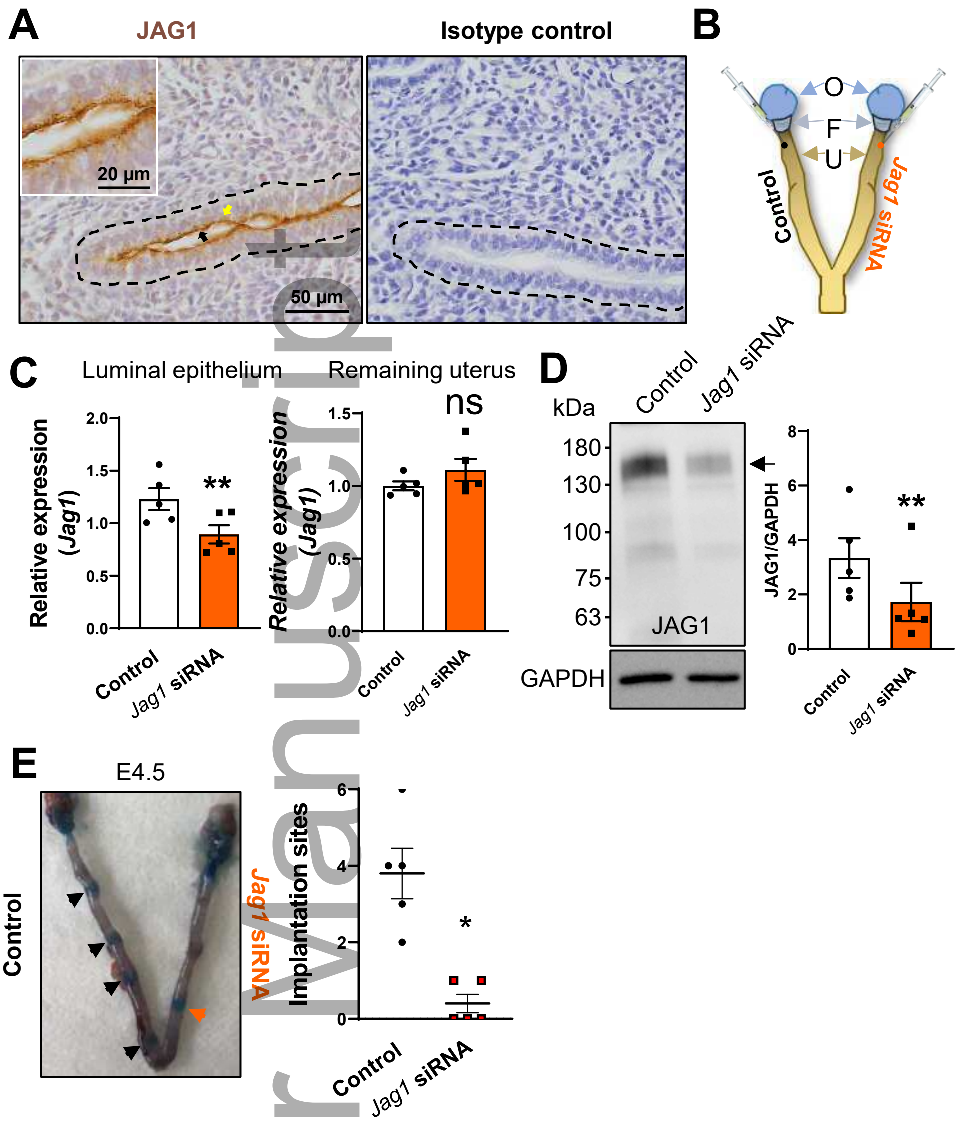
A
JAG1
20 µm
50 µm
Isotype control
B
O
F
U
Control
Jag1 siRNA
C
Luminal epithelium
Remaining uterus
Relative expression (Jag1)
2.0
1.5
1.0
0.5
0.0
**
ns
Control
Jag1 siRNA
D
kDa
Control
Jag1 siRNA
180
130
100
75
63
JAG1
GAPDH
JAG1/GAPDH
8
6
4
2
0
**
E
E4.5
Control
Jag1 siRNA
Implantation sites
6
4
2
0
*

Fig. 5

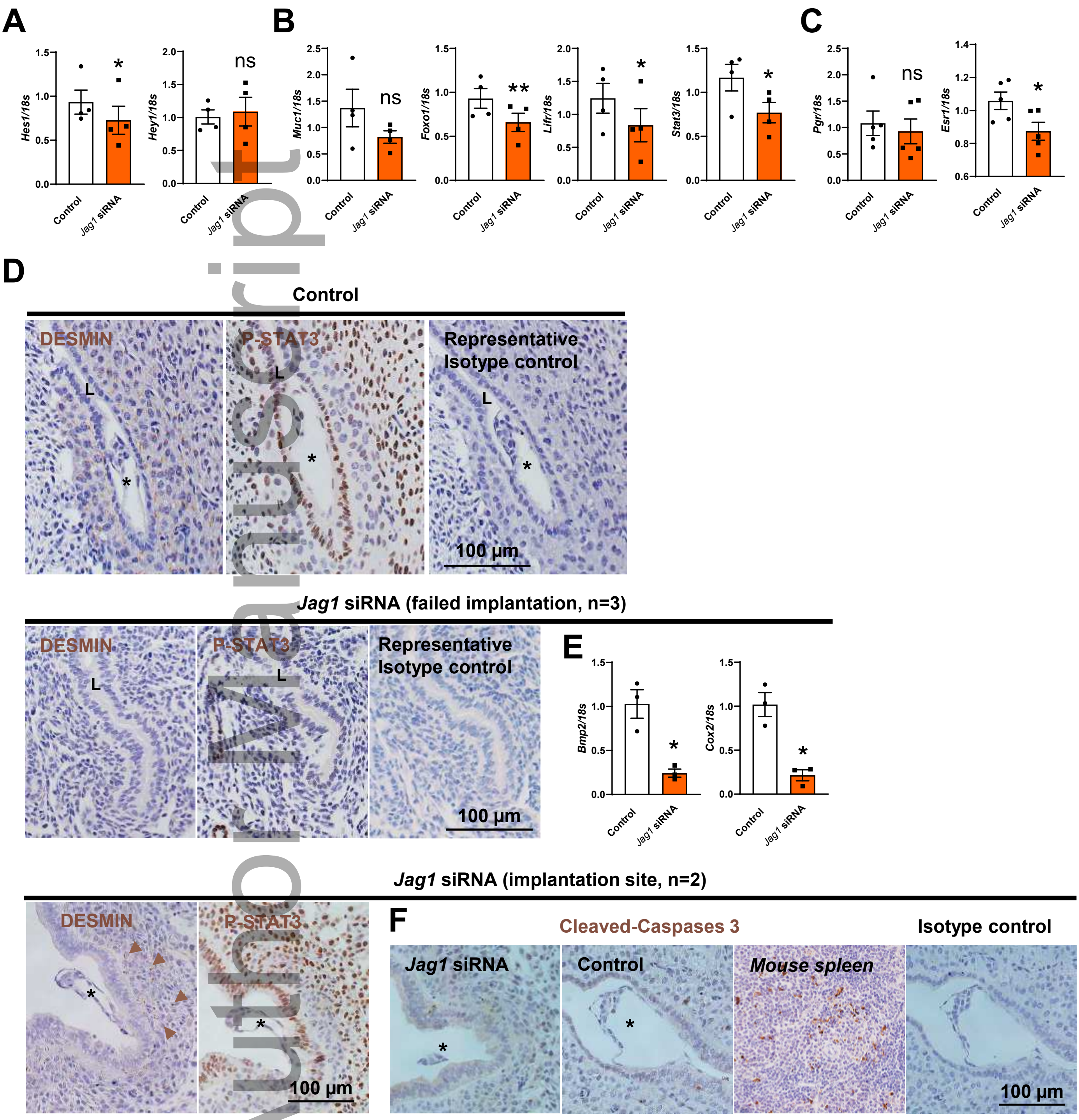
A
Hes1/18s
Hey1/18s
*
ns
B
Muc1/18s
Foxo1/18s
Lifr/18s
Stat3/18s
ns
**
*
*
C
Pgr/18s
Esr1/18s
ns
*
Control
Jag1 siRNA
D
Control
DESMIN
P-STAT3
Representative Isotype control
L
*
100 µm
Jag1 siRNA (failed implantation, n=3)
DESMIN
P-STAT3
Representative Isotype control
L
100 µm
E
Bmp2/18s
Cox2/18s
*
*
Control
Jag1 siRNA
Jag1 siRNA (implantation site, n=2)
DESMIN
P-STAT3
*
100 µm
F
Cleaved-Caspases 3
Isotype control
Jag1 siRNA
Control
Mouse spleen
*
100 µm

Fig. 6

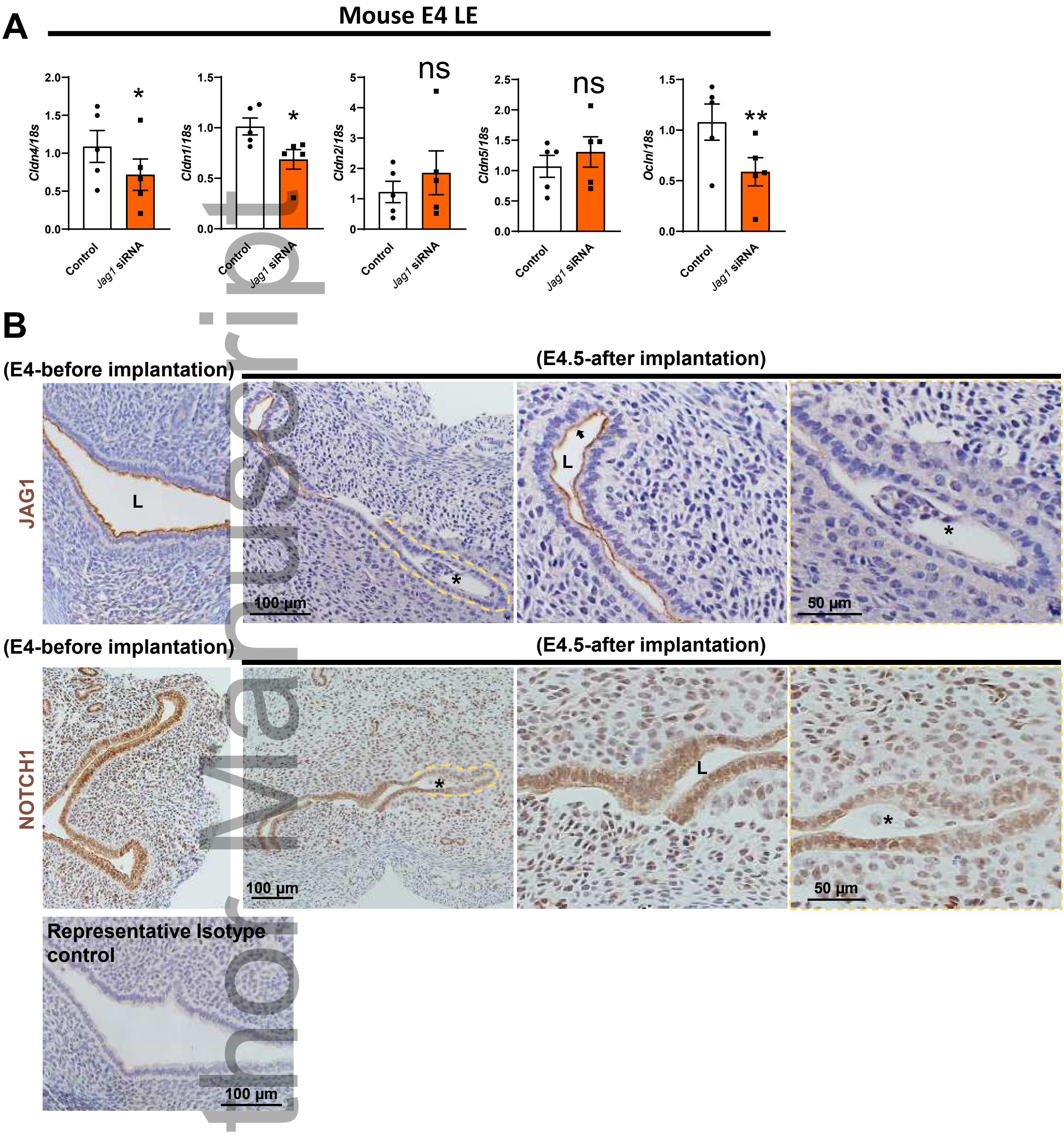
A
Mouse E4 LE
2.0
1.5
1.0
0.5
0.0
Cldn4/18s
*
Control
Jag1 siRNA
1.5
1.0
0.5
0.0
Cldn1/18s
*
Control
Jag1 siRNA
5
4
3
2
1
0
Cldn2/18s
ns
Control
Jag1 siRNA
2.5
2.0
1.5
1.0
0.5
0.0
Cldn5/18s
ns
Control
Jag1 siRNA
1.5
1.0
0.5
0.0
Ocln/18s
**
Control
Jag1 siRNA
B
(E4-before implantation)
(E4.5-after implantation)
JAG1
L
*
100 µm
L
*
50 µm
(E4-before implantation)
(E4.5-after implantation)
NOTCH1
*
100 µm
L
*
50 µm
Representative Isotype control
100 µm